HHS Public Access

Author manuscript

Prog Neuropsychopharmacol Biol Psychiatry. Author manuscript; available in PMC 2017 April 03.

Published in final edited form as:

Prog Neuropsychopharmacol Biol Psychiatry. 2016 April 3; 66: 48–53. doi:10.1016/j.pnpbp.2015.11.005.

A proton spectroscopy study of white matter in children with autism

Antonio Y. Hardan[a,*], **Lawrence K. Fung**[a], **Thomas Frazier**[b], **Sean W. Berquist**[a], **Nancy J. Minshew**[c], **Matcheri S. Keshavan**[d], and **Jeffrey A. Stanley**[e]

[a]Department of Psychiatry and Behavioral Sciences, Stanford University, Stanford, CA, USA

[b]Center for Autism and Center for Pediatric Behavioral Health, Pediatric Institute, Cleveland Clinic, Cleveland, OH, USA

[c]Department of Psychiatry, Western Psychiatric Institute and Clinic, University of Pittsburgh, Pittsburgh, PA, USA

[d]Department of Psychiatry, Beth Israel and Deaconess Medical Center, Harvard Medical School, Boston, MA, USA

[e]Department of Psychiatry and Behavioral Neurosciences, Wayne State University School of Medicine, Detroit, MI, USA

Abstract

White matter abnormalities have been described in autism spectrum disorder (ASD) with mounting evidence implicating these alterations in the pathophysiology of the aberrant connectivity reported in this disorder. The goal of this investigation is to further examine white matter structure in ASD using proton magnetic resonance spectroscopy (^{1}H MRS). Multi-voxel, short echo-time *in vivo* ^{1}H MRS data were collected from 17 male children with ASD and 17 healthy age- and gender- matched controls. Key ^{1}H metabolite ratios relative to phosphocreatine plus creatine were obtained from four different right and left white matter regions. Significantly lower N-acetylaspartate/creatine ratios were found in the anterior white matter regions of the ASD group when compared to controls. These findings reflect impairment in neuroaxonal white matter tissue and shed light on the neurobiologic underpinnings of white matter abnormalities in ASD by implicating an alteration in myelin and/or axonal development in this disorder.

Keywords

in vivo ^{1}H MRS; N-acetylaspartate (NAA); phosphocreatine plus creatine; connectivity

[*]Corresponding Author: 401 Quarry Road, Stanford, CA 94305, Phone: 1-650-724-8919, Fax: 1-650-724-7389, hardanay@stanford.edu.

1. Introduction

Autism spectrum disorder (ASD) is characterized by impairments in social interaction, communication, and stereotyped and/or repetitive behaviors (APA, 2000). ASD represents a set of etiologically heterogeneous neurodevelopmental disorders but appear to share common biologic abnormalities implicating alterations in neural connectivity, involving short- and long-distance connections potentially contributing to the development of some symptoms of ASD (Courchesne and Pierce, 2005, Just et al. , 2007). The integrity of several elements including neuronal bodies and axons as well as myelin sheath is essential to optimal connectivity between brain regions and the examination of grey and white matter (WM) structures is crucial for a better understanding of the neurobiologic underpinnings of abnormal connectivity. Recently, neuroimaging studies have focused on WM structural alterations and investigators have applied different methods including region of interest approaches and diffusion tensor imaging (DTI).

Volumetric studies have focused on discrete brain regions and have identified abnormalities in several WM structures. Herbert et al. applied a novel MRI parcellation method and showed that WM volume was increased in outer zone regions (closer to the cortical surface) with no significant differences in inner zone regions (peri-callosal) (Herbert et al. , 2004). In contrast, a recent study, using a different parcellation method, found no volumetric alterations in subjacent cortical white matter but reported reduced central white matter volume (peri-callosal) in children and adolescents with ASD (Jou et al. , 2010). Reduction in central WM volume is consistent with several studies examining corpus callosum (CC) size (Hardan et al. , 2000, Piven et al. , 1997); and a recent meta-analysis substantiating this observation (Frazier and Hardan, 2009). Interestingly, this decrease in CC size appears to be persistent over time with recent evidence showing abnormal growth trajectory (Frazier et al. , 2012). This observation is consistent with a longitudinal MRI study in very young children with ASD and reporting alterations in developmental rates in several brain regions including total WM volume (Schumann et al. , 2010). These global alterations are also concordant with volumetric abnormalities in specific white matter tracts involving the right arcuate fasciculus, and the left inferior fronto-occipital and uncinate fasciculi (Radua et al. , 2011). These converging observations provide evidence of the pervasiveness of WM volumetric alterations in ASD and the examination of the underlying neurobiology is warranted.

Similar to morphometric studies, investigations applying DTI techniques have consistently observed structural alterations in WM structures. Research studies utilizing DTI to examine microstructural properties of WM in children and adults with ASD have found alterations in fractional anisotropy (FA; coherent fiber tract directionality), as well as in mean and radial diffusivities. According to a recent review of 48 DTI studies in ASD, individuals with ASD tended to have decreased FA and increased radial diffusivity in many WM tracts of the brain, but most consistently in the CC, cingulum, and aspects of the temporal lobe (Travers et al. , 2012). An exception to the reduced FA was found in a recent investigation of very young children (ages 1.8 - 3.3 years) who revealed increased FA in several brain regions including the arcuate fasciculus and CC (Ben Bashat et al. , 2007) suggesting a possible developmental effect. More recently, a longitudinal study of children at high risk of

developing ASD revealed increased FA in several white matter tracts in infants later on diagnosed with ASD compared to the control group before 12 months of age, but decreased FA in the ASD group at 24 months (Wolff et al. , 2012). Findings from these DTI investigations indicate a pervasive pattern of WM disruption at the microstructural level and a better understanding of the neurobiologic underpinnings is needed.

The goal of this pilot investigation is to apply *in vivo* proton magnetic resonance spectroscopy (^{1}H MRS) to further examine white matter abnormalities in children and adolescents with ASD in comparison to age- and gender-matched neurotypical controls. In vivo ^{1}H MRS of the brain measures levels of N-acetylaspartate (NAA), phosphocreatine plus creatine (PCr+Cr) and glycerophosphocholine plus phosphocholine (GPC+PC) as well as glutamate and myo-inositol (mI) (Stanley et al. , 2000). NAA is synthesized in neuronal mitochondria and metabolized in oligodendrocytes providing evidence of inter-compartmental cycling between neurons and oligodendrocytes (Baslow, 2000, Nadler and Cooper, 1972, Urenjak et al. , 1993). Measurements of the PCr+Cr provide information on cellular energy metabolism with evidence indicating that Cr, after phosphorylation, is utilized as an energy reservoir in cells with high-energy demands (Sartorius et al. , 2008). PC is a precursor and GPC a breakdown product of cellular membrane phospholipids. Collectively, GPC+PC, reflects membrane synthesis and turnover associated with cellular entities such as the branching of dendrites and the formation of synapses (Dowdall et al. , 1972, Stanley et al. , 1995, Stanley, Pettegrew, 2000). Finally, mI is believed to be an essential requirement for cell growth, an osmolite, and a storage form for glucose (Govindaraju et al. , 2000) and has been proposed as a glial marker (Brand et al. , 1993). We hypothesize that NAA will be lower in ASD, compared to controls. Therefore, application of ^{1}H MRS in measuring NAA and other metabolites may be of help in elucidating the neurobiologic underpinnings of white matter abnormalities in ASD.

2. Methods

2.1. Participants

Subjects were 17 boys with ASD and 17 healthy male controls between 8 and 15 years of age. Methodology of the study was approved by the Institutional Review Board. Written informed consent and assent were obtained from the parents and participants, respectively. All subjects had a full-scale IQ (FSIQ) of greater than 70. Participants with ASD represented all consecutive referrals to a research clinic who were eligible to participate in the pilot study and able to complete the imaging procedures. The diagnosis of ASD was established through the administration of the Autism Diagnostic Interview-Revised (ADI-R) and Autism Diagnostic Observation Schedule (ADOS) (Lord et al. , 2002, Lord et al. , 1994) in addition to expert clinical evaluation. Children with autistic symptoms secondary to a specific etiology such as tuberous sclerosis or fragile X syndrome were excluded, as were potential subjects with evidence of genetic, metabolic, seizure, or infectious disorders.

Neurotypical controls were children recruited from the community through advertisements in areas socio-economically comparable to those of the families of origin of subjects with ASD. Healthy subjects were screened by face-to-face evaluations, questionnaires, telephone interviews, and observation during psychometric tests (please refer to the next section).

Individuals with a family history (first degree relatives) of any neuropsychiatric disorder, such as ASD, learning disability, affective disorders, and schizophrenia, were not included. Potential subjects with a history of birth asphyxia, head injury, or a seizure disorder were also excluded. All control subjects had a FSIQ > 70 and no learning disability as assessed by the Wide Range Achievement Test-R. Exclusions for control subjects and individuals with ASD were based on history and physical examination as well as laboratory testing when indicated.

Cognitive and behavioral phenotyping of participants included the Wechsler Intelligence Scale for Children-III (WISC-III), Social Responsiveness Scale (SRS), and Vineland Adaptive Behavior Scale (VABS). The SRS is a 65-item parent report questionnaire designed to measure the severity of ASD symptoms as they occur in natural social settings (Constantino et al. , 2003). High scores in SRS indicate more severe behavioral symptoms. The VABS is a 433-item parent report questionnaire designed to assess personal and social skills needed for everyday living (Sparrow et al. , 2005). Low scores in VABS suggest lower adaptive abilities. The WISC-III is an individually administered intelligence test for children between the ages of 6 and 16 that can be completed without reading or writing (Wechsler, 1991). The socioeconomic status (SES) of the family of origin was assessed using the Hollingshead method (Hollingshead, 1975).

Table 1 presents sample demographics and clinical characteristics. Participants with ASD and healthy controls did not differ on age or SES. However, there were significant differences in FSIQ. To more accurately estimate differences attributable to ASD diagnosis, age, SES, and FSIQ were included as covariates in mixed effects regression models. As expected, individuals with ASD showed significantly higher scores on the SRS and significantly lower scores across adaptive function domains. Scores on the diagnostic measures (ADI-R and ADOS) indicate that participants with ASD tended to have relatively high symptom levels. Finally, with the exception of one individual, all participants with ASD were taking psychotropic medications including selective serotonin reuptake inhibitors (N = 9), stimulants (N = 2), atomoxetine (N = 2), and atypical antipsychotics (N = 2). Five were taking other medications such as donepezil and buspirone.

2.2. MRI Scans and Structural Measurements

MR scans were obtained on a GE 1.5 Tesla Signa whole-body MRI system (GE Medical Systems, Milwaukee, WI). A 3D, T_1-weighted spoiled gradient recalled (SPGR) acquisition sequence was performed in the coronal plane to obtain 124 images covering the entire brain (slice thickness=1.5mm, TE = 5ms; TR = 25ms; flip angle = 40 degrees, NEX = 1; FOV = 24cm; matrix = 256 × 192). A double spin-echo sequence was also used to obtain T_2-weighted and proton density (PD) images in the coronal plane (slice thickness= 5mm; TEs= 17ms and 102ms; TR = 2,500ms; NEX = 1; FOV = 24cm; matrix = 256 × 192; total slices= 24). MRI data were identified by scan number to retain blindness and analyzed using Brain Research: Analysis of Images, Networks and Systems (BRAINS) software while applying previously published methodologies of total brain volume (TBV) measurements (Magnotta, 2002). The image processing was performed on a SGI workstation (Silicon Graphics Inc., Mountain View, CA) using the BRAINS2 (University of Iowa, Iowa City, IA, USA)

software package. The image data was normalized to standard Talairach stereotactic three-dimensional space (Talairach and Tournoux, 1988) by identifying six brain-limiting points (anterior, posterior, superior, inferior, left, and right); the anterior-posterior commissure line specified the x-axis, a vertical line rising from the x-axis through the interhemispheric fissure specified the y-axis, and a transverse orthogonal line with respect to x and y coordinates specified the z-axis. Registration was performed by aligning the T_2-weighted and PD images with a resampled T_1-weighted image and then resampling the T_2-weighted and PD images themselves (Magnotta, 2002). After normalization to a standard three-dimensional space, the pixels representing grey matter, white matter, and cerebrospinal fluid were identified using a segmentation algorithm applied to the T_1-weighted, T_2-weighted and PD image sequences as described elsewhere (White et al. , 2003).

2.3. ^{1}H Spectroscopy

A 2D, multi-voxel ^{1}H spectroscopy acquisition method was applied here combining the stimulated echo acquisition mode (STEAM) sequence (Frahm et al. , 1989) with the phase encoding steps of chemical shift imaging (CSI), which is termed STEAM CSI on the GE system. This sequence is similar to the GE ProbeSI sequence. The STEAM sequence localized a 3D region of interest (ROI) with an axial thickness of 20 mm and right/left and anterior/posterior dimensions of approximately 100 mm × 80 mm to ensure the CSI signal was within the cerebrum. The ROI in the axial direction was parallel to the anterior commissure-posterior commissure (AC-PC) line and its inferior limit was at the superior edge of the orbital bone resulting in an ROI encompassing the right and left thalami. Acquisition parameters included a repetition time TR of 1.6 s, TE of 20 ms, TM of 13.7 ms, FOV of 24 cm, 16 ×16 phase encoding steps or 16 × 16 voxels with a nominal voxel size of 15 × 15 × 20 mm^3, 1,024 complex data points, 2.5 kHz spectral bandwidth, and 4 averages. A water-unsuppressed measurement was also collected with 8 × 8 phase encoding steps.

As part of the post-processing, the CSI was repositioned, in each subject, by shifting the 16 × 16 voxel grid in the right/left and anterior/posterior directions, prior to the 2D inverse Fourier transformation (IFT) to ensure that voxels were centered in the following right and left brain regions: anterior frontal white matter, anterior middle centrum semiovale, posterior middle centrum semiovale and posterior parietal white matter (see Fig. 1 for naming of voxels). Voxels in the middle centrum semiovale were more specifically located superior to the anterior and retrolenticular limbs of the internal capsule, respectively. In conjunction with the grid shift, a mild spatial apodization (i.e., Fermi window with 90% diameter and 5% transition width) was applied followed by the 2D IFT. Based on empirical calculations of the point spread of a 16 × 16 CSI matrix with a mild apodization, the effective voxel size was 28% greater than the nominal size (i.e. 1.7 × 1.7 × 2.0 cm^3 or 5.8 cm^3). The determination of the effective voxel size was based on the finite sampling of the CSI (Hetherington et al. , 1994), and this voxel size was applied to all voxels. For each right and left voxels, no apodization was applied to the signal and the quantification of the spectral metabolites NAA, mI, PCr+Cr, GPC+PC, taurine, alanine, aspartate, gamma amino-butyric acid (GABA), glucose, and N-acetylaspartylglutamate (NAAG), as well as lipid resonances and macromolecule resonances (Seeger et al. , 2003), was done using the Linear Combination (LC) Model software version 6.1-4 (Provencher, 1993). Only results of the

more reliable measures (NAA, PCr+Cr, GPC+PC, and mI) were used in the analysis. Ratios of metabolites relative to PCr+Cr were generated. Cramér-Rao lower bound (CLRB) of 20 is set as the threshold for data inclusion.

2.4. Analytic Plan

Separate mixed effects regression models were computed to examine diagnostic group differences in each MRS metabolite measure. Diagnostic Group (ASD vs. healthy controls) was a fixed-effects factor. Hemisphere (left vs. right) and regions (See Fig. 1 for naming of regions R1, R2, R3, and R4) served as repeated measures variables. FSIQ, and age were included as covariates. SES will also be used as a covariate since greater early life socioeconomic deprivation was found to associate with lower concentrations of NAA (McLean et al. , 2012). For these preliminary analyses, a significant Diagnostic Group main effect would indicate overall differences between ASD and control cases. Main effects for Hemisphere and Lobe would indicate metabolite differences across brain regions, irrespective of diagnostic group. A significant interaction between Diagnostic Group and Hemisphere or Lobe would indicate differences in the pattern of metabolite levels between ASD and control cases across brain hemispheres/regions.

Mixed effects regression models are advantageous in that they accommodate missing data. Model fit was considered by iteratively examining random effects and alternative covariance structures (Kreft, 1995, Peugh and Enders, 2005, Raudenbush and Bryk, 2002). A simple diagonal covariance structure fits equally well or better to other structures. Results are presented with covariate adjustment (age, SES, FSIQ) to more precisely estimate group differences in metabolites. F-tests for the main effects and interactions in the above mixed effects regression models were converted to Cohen's d to examine the magnitude of these effects. Conventions for interpretation of Cohen's d are small (d=.20), medium (d=.50), and large (d=.80). The effect size of the main effect of Diagnostic Group gives the magnitude of overall metabolite differences between ASD and control cases. Metabolites were examined as ratios (i.e., relative to PCr+Cr).

3. Results

Table 2 shows metabolite/PCr+Cr ratio levels for ASD and control participants. Analyzing all white matter voxels together, NAA ratios were lower in participants with ASD when compared to controls ($p = .042$; $d = -.77$). The average (±standard deviation) CLRB's range from 8.8 (±2.4) to 10.3 (±3.4) for NAA, from 13.2 (±3.6) to 15.6 (±4.1) for mI, from 10.1 (±2.9) to 11.2 (±2.9) for GPC+PC, and from 9.3 (±2.7) to 11.3 (±3.2) for PCr+Cr. Decreased NAA/PCr+Cr levels were also observed in the anterior frontal white matter ($p = .022$; $d = -.52$) and anterior middle centrum semiovale ($p = .042$; $d = -.46$). Finally, analyses were also completed using absolute quantification, and revealed consistent findings with regards to NAA (see supplemental information; Table 3). Interestingly, additional differences were found in other absolute metabolite levels that were not detected in the ratio analysis.

4. Discussion

NAA is present at high concentration in the brain and is viewed as a marker of functioning neuroaxonal tissue that includes functional aspects of the formation and maintenance of myelin (Chakraborty et al. , 2001). In the present study, decreased NAA/PCr+Cr ratios, as measured by ^{1}H MRS, were observed primarily in the rostral regions of white matter of children and young adolescents with ASD compared to controls. This finding implies the existence of an alteration in the neuroaxonal functioning of WM potentially implicating altered development of myelin in ASD. These MRS findings are consistent with numerous prior investigations reporting WM abnormalities in ASD that utilized volumetric and DTI methods. Over the last two decades a series of studies have reported on structural alterations of WM in ASD describing possible increases in the WM volumes in cortical regions (Carper et al. , 2002), in contrast to a decrease in the volume in callosal and pericallosal regions (Chung et al. , 2004, Frazier and Hardan, 2009, Herbert, Ziegler, 2004). Similarly, abnormalities in DTI measures have consistently been reported with decreased fractional anisotropy in several key WM tracts including several regions described here such as frontal lobe (Shukla et al. , 2011a, Sundaram et al. , 2008) as well as the anterior and posterior limbs of the internal capsule (Cheng et al. , 2010, Shukla et al. , 2011b).

Findings from the current study are consistent with some (Friedman et al. , 2003, Levitt et al. , 2003) but not all (DeVito et al. , 2007, Fayed and Modrego, 2005) previously reported ^{1}H MRS investigations examining WM structures in children with ASD. Freidman et al. acquired ^{1}H MRS scans from forty-five 3 and 4 year old children with ASD, 15 age-matched children with developmental delay, and 13 age-matched typically developing children (Friedman, Shaw, 2003). CSI revealed lower levels of NAA in the left frontal and right parietal WM (but not CC) in both children with ASD and children with developmental delay when compared to typically developing children. In another study, Levitt et al applied ^{1}H MRS imaging in 22 children and adolescents with ASD (age range 5 to 16 years) and 20 age-matched typically developing control subjects to investigate potential between-group differences in levels of metabolites in several brain regions including WM (Levitt, O'Neill, 2003). Using single-voxel spectroscopy (SVS), decreased levels of NAA were observed in the left (but not the right) frontal and parietal WM regions in this sample of children and adolescents with ASD (Levitt, O'Neill, 2003). In contrast, using partial regression volume analysis, DeVito et al. did not find any differences in the ^{1}H metabolite levels including NAA in the cerebral WM between 26 males with ASD (age range 6 to 17 years) and 29 age-matched male controls. Finally, using an ROI approach with SVS Fayed et al. examined the left centrum semiovale of 21 children with ASD, 8 with attention-deficit hyperactivity disorder, and 12 neurotypical controls, and found no difference between the ASD and the control groups (Fayed and Modrego, 2005). Taken together, the most consistent finding from the present study and previous investigations (Friedman, Shaw, 2003, Levitt, O'Neill, 2003) is the decreased NAA levels in both frontal and parietal WM. However, reduced NAA levels in anterior centrum semiovale in the present study is not supported by findings by Fayed et al. (Fayed and Modrego, 2005). This discrepancy may be due to the choice of the ROI – in the present study, the anterior and posterior portions of the middle centrum semiovale were sampled separately, and we averaged the left and right parts

of each of these structures; in contrast, Fayed et al. examined the full centrum semiovale but only on the left side. In addition to the selection of brain regions examined, differences in methods of acquisition and analysis, as well as characteristics of participants (gender, age range) might also contribute to inconsistent results.

NAA is present at high concentration in the brain and has traditionally been linked to neuronal dysfunction, and axonal loss, with recent evidence supporting its role in myelin lipid metabolism since it serves as a critical source of acetate for lipid synthesis in oligodendrocytes and subsequent myelination (Moffett et al. , 2007). Lower NAA levels in WM has been observed in several brain disorders (Moffett, Ross, 2007) such as acute traumatic brain injury, brain ischemia, Alzheimer's disease and multiple sclerosis (Danielsen and Ross, 1999). Psychoactive compounds can also reduce brain NAA levels, including atomoxetine treatment (Husarova et al. , 2014) and after ingestion of ethanol or alcohol dehydrogenase inhibitors (Baslow, 2000). Therefore, decreased NAA levels in WM structures observed in the current sample could be related to axonal dysfunction, myelin pathology, psychotropic treatment, or all of them. The exact pathophysiology remains to be elucidated.

The current study contains several methodological limitations. The sample size was relatively small and included only males with a wide age range. Most subjects were taking psychotropic medications known to affect levels of metabolites. Additionally, the ^{1}H spectroscopy acquisition and data processing are limited by the use of a low magnetic field strength and lack of accounting for tissue composition including cerebrospinal fluid correction (Hardan et al. , 2008). Finally, using ratios to Cr+PCr might not be ideal since these metabolites might also be affected by disease state. Therefore, absolute values are included in the supplemental material.

In conclusion, evidence from this preliminary study point to the existence of pervasive alterations of ^{1}H metabolites in white matter regions in children with ASD as measured by ^{1}H MRS. The reduced NAA/PCr+Cr ratios primarily in the anterior portion of the WM is consistent with several ^{1}H MRS studies examining WM regions (Friedman, Shaw, 2003, Levitt, O'Neill, 2003), thus further implicating the relevance of WM in the pathophysiology of ASD. Future ^{1}H MRS studies are warranted to comprehensively examine the relationship between WM NAA alterations and clinical features and, more importantly, to further our understanding of the physiology of the different metabolites in ASD.

Supplementary Material

Refer to Web version on PubMed Central for supplementary material.

Acknowledgments

This work was supported by NIMH grant MH 64027 (AYH). The efforts and commitment of the participants and their families in this study are gratefully acknowledged.

Abbreviations

AC-PC	anterior commissure-posterior commissure
CSI	chemical shift imaging
CC	corpus callosum
Cr	creatine
DTI	diffusion tensor imaging
FA	fractional anisotropy
FSIQ	full-scale intelligence quotient
GABA	gamma amino-butyric acid
GPC	glycerophosphocholine
^{1}H MRS	proton magnetic resonance spectroscopy
IFT	inverse Fourier transformation
mI	myo-inositol
NAA	N-acetylaspartate
PC	phosphocholine
PCr	phosphocreatine
PD	proton density
SES	socio-economic status
STEAM	stimulated echo acquisition mode
TBV	total brain volume
WM	white matter

References

APA. Diagnostic and statistical manual of mental disorders: DSM-IV. 4th ed. American Psychiatric Association; Washington, DC: 2000.

Baslow MH. Functions of N-acetyl-L-aspartate and N-acetyl-L-aspartylglutamate in the vertebrate brain: role in glial cell-specific signaling. J Neurochem. 2000; 75:453–9. [PubMed: 10899919]

Baslow MH. Evidence supporting a role for N-acetyl-L-aspartate as a molecular water pump in myelinated neurons in the central nervous system. An analytical review. Neurochem Int. 2002; 40:295–300. [PubMed: 11792458]

Ben Bashat D, Kronfeld-Duenias V, Zachor DA, Ekstein PM, Hendler T, Tarrasch R, et al. Accelerated maturation of white matter in young children with autism: a high b value DWI study. Neuroimage. 2007; 37:40–7. [PubMed: 17566764]

Brand A, Richter-Landsberg C, Leibfritz D. Multinuclear NMR studies on the energy metabolism of glial and neuronal cells. Dev Neurosci. 1993; 15:289–98. [PubMed: 7805581]

Carper RA, Moses P, Tigue ZD, Courchesne E. Cerebral lobes in autism: early hyperplasia and abnormal age effects. Neuroimage. 2002; 16:1038–51. [PubMed: 12202091]

Chakraborty G, Mekala P, Yahya D, Wu G, Ledeen RW. Intraneuronal N-acetylaspartate supplies acetyl groups for myelin lipid synthesis: evidence for myelin-associated aspartoacylase. J Neurochem. 2001; 78:736–45. [PubMed: 11520894]

Cheng Y, Chou KH, Chen IY, Fan YT, Decety J, Lin CP. Atypical development of white matter microstructure in adolescents with autism spectrum disorders. Neuroimage. 2010; 50:873–82. [PubMed: 20074650]

Chung MK, Dalton KM, Alexander AL, Davidson RJ. Less white matter concentration in autism: 2D voxel-based morphometry. Neuroimage. 2004; 23:242–51. [PubMed: 15325371]

Constantino JN, Davis SA, Todd RD, Schindler MK, Gross MM, Brophy SL, et al. Validation of a brief quantitative measure of autistic traits: comparison of the social responsiveness scale with the autism diagnostic interview-revised. J Autism Dev Disord. 2003; 33:427–33. [PubMed: 12959421]

Courchesne E, Pierce K. Brain overgrowth in autism during a critical time in development: implications for frontal pyramidal neuron and interneuron development and connectivity. Int J Dev Neurosci. 2005; 23:153–70. [PubMed: 15749242]

Danielsen, ER.; Ross, B. Magnetic resonance spectroscopy diagnosis of neurological diseases. Marcel Dekker Inc.; New York: 1999.

DeVito TJ, Drost DJ, Neufeld RW, Rajakumar N, Pavlosky W, Williamson P, et al. Evidence for cortical dysfunction in autism: a proton magnetic resonance spectroscopic imaging study. Biol Psychiatry. 2007; 61:465–73. [PubMed: 17276747]

Dowdall MJ, Barker LA, Whittaker VP. Choline metabolism in the cerebral cortex of guinea pigs. Phosphorylcholine and lipid choline. Biochem J. 1972; 130:1081–94. [PubMed: 4656795]

Erecinska M, Silver IA. Metabolism and role of glutamate in mammalian brain. Prog Neurobiol. 1990; 35:245–96. [PubMed: 1980745]

Fayed N, Modrego PJ. Comparative study of cerebral white matter in autism and attention-deficit/hyperactivity disorder by means of magnetic resonance spectroscopy. Academic radiology. 2005; 12:566–9. [PubMed: 15866128]

Frahm, J.; Hanicke, W.; Merboldt, K. Method for rapid acquisition of spin resonance data for a spatially resolved investigation of an object. United States: 1989.

Frazier TW, Hardan AY. A meta-analysis of the corpus callosum in autism. Biol Psychiatry. 2009; 66:935–41. [PubMed: 19748080]

Frazier TW, Keshavan MS, Minshew NJ, Hardan AY. A two-year longitudinal MRI study of the corpus callosum in autism. J Autism Dev Disord. 2012; 42:2312–22. [PubMed: 22350341]

Friedman SD, Shaw DW, Artru AA, Richards TL, Gardner J, Dawson G, et al. Regional brain chemical alterations in young children with autism spectrum disorder. Neurology. 2003; 60:100–7. [PubMed: 12525726]

Govindaraju V, Young K, Maudsley AA. Proton NMR chemical shifts and coupling constants for brain metabolites. NMR Biomed. 2000; 13:129–53. [PubMed: 10861994]

Hardan AY, Minshew NJ, Keshavan MS. Corpus callosum size in autism. Neurology. 2000; 55:1033–6. [PubMed: 11061265]

Hardan AY, Minshew NJ, Melhem NM, Srihari S, Jo B, Bansal R, et al. An MRI and proton spectroscopy study of the thalamus in children with autism. Psychiatry research. 2008; 163:97–105. [PubMed: 18508243]

Herbert MR, Ziegler DA, Makris N, Filipek PA, Kemper TL, Normandin JJ, et al. Localization of white matter volume increase in autism and developmental language disorder. Ann Neurol. 2004; 55:530–40. [PubMed: 15048892]

Hetherington HP, Mason GF, Pan JW, Ponder SL, Vaughan JT, Twieg DB, et al. Evaluation of cerebral gray and white matter metabolite differences by spectroscopic imaging at 4.1T. Magn Reson Med. 1994; 32:565–71. [PubMed: 7808257]

Hollingshead, A. Four Factor Index of Social Status. Yale University; New Haven, CT: 1975.

Husarova V, Bittsansky M, Ondrejka I, Dobrota D. Prefrontal grey and white matter neurometabolite changes after atomoxetine and methylphenidate in children with attention deficit/hyperactivity disorder: a (1)H magnetic resonance spectroscopy study. Psychiatry Res. 2014; 222:75–83. [PubMed: 24679996]

Jou RJ, Minshew NJ, Keshavan MS, Hardan AY. Cortical gyrification in autistic and Asperger disorders: a preliminary magnetic resonance imaging study. J Child Neurol. 2010; 25:1462–7. [PubMed: 20413799]

Just MA, Cherkassky VL, Keller TA, Kana RK, Minshew NJ. Functional and anatomical cortical underconnectivity in autism: evidence from an FMRI study of an executive function task and corpus callosum morphometry. Cereb Cortex. 2007; 17:951–61. [PubMed: 16772313]

Kreft IG. Special Issue: Hierarchical Linear Models: Problems and Prospects. Journal of Educational and Behavioral Statistics. 1995; 20:109–13.

Levitt JG, O'Neill J, Blanton RE, Smalley S, Fadale D, McCracken JT, et al. Proton magnetic resonance spectroscopic imaging of the brain in childhood autism. Biol Psychiatry. 2003; 54:1355–66. [PubMed: 14675799]

Lord, C.; Rutter, M.; DiLavore, P.; Risi, S. Autism Diagnostic Observation Schedule (ADOS). Western Psychological Services; Los Angeles, CA: 2002.

Lord C, Rutter M, Le Couteur A. Autism Diagnostic Interview-Revised: a revised version of a diagnostic interview for caregivers of individuals with possible pervasive developmental disorders. J Autism Dev Disord. 1994; 24:659–85. [PubMed: 7814313]

Magnotta V. Structural MR image processing using the BRAINS2 toolbox. Comput Med Imag Grap. 2002; 26:251.

McLean J, Krishnadas R, Batty GD, Burns H, Deans KA, Ford I, et al. Early life socioeconomic status, chronic physiological stress and hippocampal N-acetyl aspartate concentrations. Behavioural brain research. 2012; 235:225–30. [PubMed: 22917526]

Moffett JR, Ross B, Arun P, Madhavarao CN, Namboodiri AM. N-Acetylaspartate in the CNS: from neurodiagnostics to neurobiology. Prog Neurobiol. 2007; 81:89–131. [PubMed: 17275978]

Nadler JV, Cooper JR. N-acetyl-L-aspartic acid content of human neural tumours and bovine peripheral nervous tissues. J Neurochem. 1972; 19:313–9. [PubMed: 4334499]

Peugh, JL.; Enders, CK. Using the SPSS Mixed Procedure to Fit Cross-Sectional and Longitudinal Multilevel Models. Educational and Psychological Measurement; 2005.

Piven J, Bailey J, Ranson BJ, Arndt S. An MRI study of the corpus callosum in autism. Am J Psychiatry. 1997; 154:1051–6. [PubMed: 9247388]

Provencher S. Estimation of metabolite concentrations from localized in vivo proton NMR spectra. Magnetic resonance in medicine: official journal of the Society of Magnetic Resonance in Medicine/Society of Magnetic Resonance in Medicine. 1993; 30:672.

Radua J, Via E, Catani M, Mataix-Cols D. Voxel-based meta-analysis of regional white-matter volume differences in autism spectrum disorder versus healthy controls. Psychol Med. 2011; 41:1539–50. [PubMed: 21078227]

Raudenbush, SW.; Bryk, AS. Hierarchical linear models: applications and data analysis methods. Second ed. Sage Pubications, Inc; Thousand Oaks, California: 2002.

Rubenstein JL, Merzenich MM. Model of autism: increased ratio of excitation/inhibition in key neural systems. Genes Brain Behav. 2003; 2:255–67. [PubMed: 14606691]

Sartorius A, Lugenbiel P, Mahlstedt MM, Ende G, Schloss P, Vollmayr B. Proton magnetic resonance spectroscopic creatine correlates with creatine transporter protein density in rat brain. J Neurosci Methods. 2008; 172:215–9. [PubMed: 18555535]

Schumann CM, Bloss CS, Barnes CC, Wideman GM, Carper RA, Akshoomoff N, et al. Longitudinal magnetic resonance imaging study of cortical development through early childhood in autism. J Neurosci. 2010; 30:4419–27. [PubMed: 20335478]

Seeger U, Klose U, Mader I, Grodd W, Nägele T. Parameterized evaluation of macromolecules and lipids in proton MR spectroscopy of brain diseases. Magnetic resonance in medicine: official journal of the Society of Magnetic Resonance in Medicine/Society of Magnetic Resonance in Medicine. 2003; 49:19.

Shukla DK, Keehn B, Muller RA. Tract-specific analyses of diffusion tensor imaging show widespread white matter compromise in autism spectrum disorder. J Child Psychol Psychiatry. 2011a; 52:286–95. [PubMed: 21073464]

Shukla DK, Keehn B, Smylie DM, Muller RA. Microstructural abnormalities of short-distance white matter tracts in autism spectrum disorder. Neuropsychologia. 2011b; 49:1378–82. [PubMed: 21333661]

Sparrow, S.; Balla, DA.; Cinchetti, D. Vineland Adaptive Behavior Scales. Pearson Education, Inc.; Bloomington, IN: 2005.

Stanley JA, Drost DJ, Williamson PC, Thompson RT. The use of a priori knowledge to quantify short echo in vivo 1H MR spectra. Magn Reson Med. 1995; 34:17–24. [PubMed: 7674893]

Stanley JA, Pettegrew JW, Keshavan MS. Magnetic resonance spectroscopy in schizophrenia: methodological issues and findings--part I. Biol Psychiatry. 2000; 48:357–68. [PubMed: 10978719]

Sundaram SK, Kumar A, Makki MI, Behen ME, Chugani HT, Chugani DC. Diffusion tensor imaging of frontal lobe in autism spectrum disorder. Cereb Cortex. 2008; 18:2659–65. [PubMed: 18359780]

Talairach, J.; Tournoux, P. Co-planar stereotaxic atlas of the human brain. Thieme, Stuttgart: 1988.

Travers BG, Adluru N, Ennis C, Tromp do PM, Destiche D, Doran S, et al. Diffusion tensor imaging in autism spectrum disorder: a review. Autism Res. 2012; 5:289–313. [PubMed: 22786754]

Urenjak J, Williams SR, Gadian DG, Noble M. Proton nuclear magnetic resonance spectroscopy unambiguously identifies different neural cell types. J Neurosci. 1993; 13:981–9. [PubMed: 8441018]

Wechsler, D. WISC-III: Wechsler intelligence scale for children. Psychological Corporation; San Antonio, TX: 1991.

White T, Andreasen NC, Nopoulos P, Magnotta V. Gyrification abnormalities in childhood- and adolescent-onset schizophrenia. Biol Psychiatry. 2003; 54:418–26. [PubMed: 12915286]

Wolff JJ, Gu H, Gerig G, Elison JT, Styner M, Gouttard S, et al. Differences in white matter fiber tract development present from 6 to 24 months in infants with autism. Am J Psychiatry. 2012; 169:589–600. [PubMed: 22362397]

Highlights

- Multi-voxel ^{1}H MRS was conducted in male children with ASD.
- Lower NAA/Cr ratios were found in anterior white matter regions of the ASD group.
- Impairment in neuroaxonal white matter may be part of the pathology of ASD.

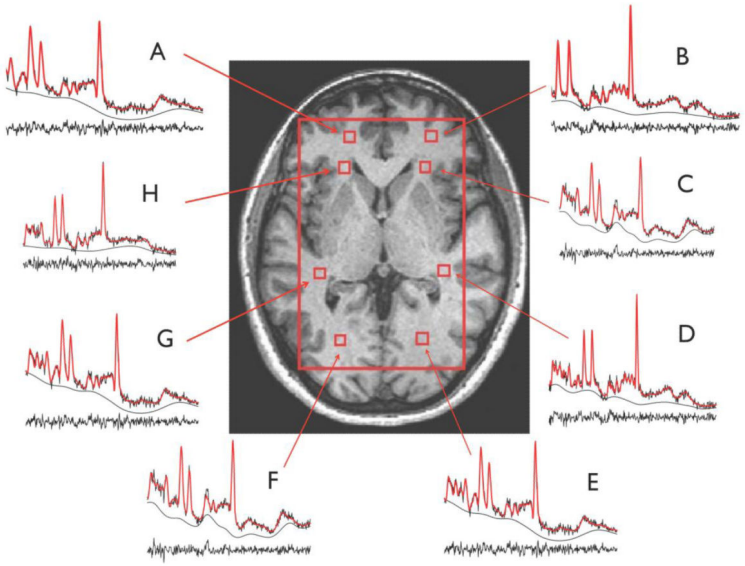

Figure 1.

White matter voxel localizations and representative quantified ^{1}H MRS spectra of the 4 right and left brain regions: Region 1 (R1; A and B): anterior frontal white matter regions; Region 2 (R2; C and H): anterior middle centrum semiovale; Region 3 (R3; D and G): posterior middle centrum semiovale; Region 4 (R4; E and F): posterior parietal white matter.

Table 1

Sample Demographics and Clinical Characteristics.

	ASD Mean (SD)	Controls Mean (SD)	t	p
N	17	17		
Age	12.5 (1.9)	11.6 (1.2)	1.68	.103
SES	4.5 (0.6)	4.4 (0.5)	0.60	.551
FSIQ	93.5 (18.3)	119.8 (11.3)	5.06	<.001
SRS Total (T-score*)	84.1 (11.1)	41.1 (3.0)	14.04	<.001
Vineland (SS#)				
Communication	94.2 (15.7)	104.9 (10.6)	2.31	.028
ADLs	80 (23.0)	102.6 (9.5)	3.74	.001
Social	76.2 (22.4)	107.3 (9.5)	5.25	<.001
Composite	81.3 (21.3)	106.5 (10.1)	4.37	<.001
ADI-R Total	50.7 (8.3)			
ADOS Total	15.3 (3.2)			

ASD: Autism spectrum disorder;

*T-score = Mean of 50 and a standard deviation of 10.

#SS=Standard Score with mean of 100 and a standard deviation of 15.

Abbreviations: ADLs, activities of daily living; FSIQ, full scale intelligence quotient; SD, standard deviation; SES, socioeconomic status; Vineland, Vineland adaptive behavior scale.

Table 2

^{1}H metabolite ratios overall and regionally of children with autism spectrum disorder and neurotypical controls

	ASD (N=17)	Controls (N=17)		Diagnostic Group	
	M (SE)	M (SE)	F	(p)	Cohen's d
Overall					
NAA/PCr+Cr	1.49 (.05)	1.64 (.05)	4.94	(.042)	−.77
GPC+PC/PCr+Cr	0.36 (.01)	0.35 (.01)	0.50	(.485)	.26
mI/PCr+Cr	0.98 (.04)	0.95 (.03)	0.36	(.553)	.22
Brain Regions **Anterior frontal WM (R1)**					
NAA/PCr+Cr	1.38 (.07)	1.60 (.06)	5.48	(.022)	−.52
GPC+PC/PCr+Cr	0.33 (.02)	0.37 (.02)	2.22	(.140)	−.33
mI/PCr+Cr	1.01 (.06)	0.92 (.06)	1.25	(.268)	.25
Anterior Middle Centrum semiovale WM (R2)					
NAA/PCr+Cr	1.42 (.06)	1.59 (.06)	4.24	(.042)	−.46
GPC+PC/PCr+Cr	0.38 (.02)	0.35 (.02)	1.37	(.246)	.26
mI/PCr+Cr	0.91 (.05)	0.91 (.05)	0.01	(.993)	.00
Posterior Middle Centrum Semiovale WM (R3)					
NAA/PCr+Cr	1.53 (.06)	1.61 (.06)	0.96	(.332)	−.22
GPC+PC/PCr+Cr	0.35 (.02)	0.33 (.02)	0.66	(.422)	.18
mI/PCr+Cr	0.94 (.05)	0.87 (.05)	1.00	(.320)	.22
Posterior Parietal WM (R4)					
NAA/PCr+Cr	1.65 (.06)	1.74 (.06)	1.04	(.312)	−.23
GPC+PC/PCr+Cr	0.37 (.02)	0.36 (.02)	0.11	(.744)	.07
mI/PCr+Cr	1.04 (.05)	1.12 (.05)	0.88	(.352)	−.21

Means and standard error are adjusted for covariates (age, full-scale IQ, and SES) using mixed effects regression models. Cohen's d conventions: small (d~.20), medium (d~.50), large (d~.80). Abbreviations: ASD, autism spectrum disorder; Cr, creatine; GPC, glycerophosphocholine; mI, myo-inositol; NAA, N-acetylaspartate; PC, phosphocholine; PCr, phosphocreatine; WM, white matter